[4]K. S. Singwi, A. Sjölander, M. P. Tosi, and R. H. Land, Phys. Rev. B **1**, 1044 (1970).
[5]P. Vashishta and K. S. Singwi, Phys. Rev. B **6**, 875 (1972); Phys. Rev. B **6**, 4883 (1972).
[6]P. Nozierès and D. Pines, Phys. Rev. **111**, 442 (1958).
[7]H. Kanazawa, S. Misawa, and E. Figita, Prog. Theor. Phys. **23**, 426 (1960).
[8]P. Nozières, *Theory of Interacting Fermi System* (Benjamin, New York, 1964).
[9]D. Des Cloizeaux, *Theory of Condensed Matter* (International Atomic Energy Agency, Vienna, 1968), p. 325.
[10]R. Bansal, M. P. Khanna, and K. N. Pathak (unpublished).
[11]L. Hedin and S. Lundqvist, *Solid State Physics,* edited by F. Seitz and D. Turnbull (Academic, New York, 1969), Vol. 23.
[12]F. Toigo and T. O. Woodruff, Phys. Rev. B **2**, 3958 (1970); Phys. Rev. B **4**, 371 (1971).
[13]R. A. Ferrell, Phys. Rev. Lett. **1**, 443 (1958).
[14]J. Hubbard, Proc. R. Soc. Lond. **A243**, 336 (1957).
[15]D. J. W. Geldart and R. Taylor, Solid State Commun. **9**, 7 (1971).

PHYSICAL REVIEW B VOLUME 7, NUMBER 8 15 APRIL 1973

Impurity Diamagnetism in Metals*

C. P. Flynn and J. A. Rigert†
Physics Department and Materials Research Laboratory, University of Illinois, Urbana, Illinois 61801
(Received 31 October 1972)

The results of a broad experimental survey of impurity magnetism in liquid monovalent metal solvents is reported. As the impurity valence Z is increased, a giant impurity diamagnetism ~ -150 cm^3/mole emerges in alkali-metal solvents for $Z \sim 5$. The diamagnetism is explained by the concept of impurity ionicity developed in this paper, and the impurity structure is analyzed in detail using the present results and earlier spin-flip-scattering results of Slichter and his co-workers. There is quantitative agreement between the theory of fully ionic impurities and the experimental susceptibilities for higher-valence impurities. The broad scheme of impurity structure in monovalent metals is also clearly revealed. The susceptibility of Sn is studied as a function of host-electron density, and the transition from band to resonant $5p$ orbitals is identified. A solubility dip occurs, but the data are not precise enough to determine whether the transition has a one-electron or configurational character. It is further reported that the large diamagnetism of positive-valence solutes in Ag, previously studied by Henry and Rogers, disappears at the melting transition. No detailed analysis of this striking effect has been attempted, but the anomalous impurity diamagnetism in the solid is clearly associated with orbits involving the [111] necks on the Fermi surface.

I. INTRODUCTION

The nature of impurity states in metals has challenged experimental and theoretical investigations for fifty or more years. Much recent effort has been directed towards the study of transition-metal impurities, having unfilled d or f shells, in both "simple" metals and in more complex transition-metal host lattices. However, there remain major unresolved difficulties in our present understanding of valence impurities. These less complex solutes differ (in the atomic state) from host atoms only by the presence of extra neutralizing valence electrons. The difficulties relate to the emergence of bound impurity states, to the occurrence of ionicity among impurities in metals, and to certain striking phenomena connected with impurity diamagnetism and conduction-electron-spin resonance in metals. The central problem lies in the theoretical prediction and the experimental assignment of electronic structures to impurities in metals. In this paper we present the results of broad experimental studies, and their theoretical interpretations. These yield a substantially more complete insight into the structure of valence impurities in simple metallic solvents. Preliminary accounts of several aspects of this work have been published elsewhere.[1]

It has, of course, been understood since the pioneering work of Mott[2] that an impurity in solution must be neutralized by the electron gas, simply because metals conduct. The precise structure of the screening charge has, nevertheless, eluded description in most cases.[3] From an experimental viewpoint there is the difficulty that the impurity structure must be defined throughout the range of host band energies and below, whereas most experiments are sensitive to a limited span of energies often near the Fermi energy E_F. There are also formidable theoretical difficulties. Foremost is the problem of self-consistency: The wave function of each electron in the system must be consistent with those of the remaining electrons, in the presence of the impurity perturbation. In the one-electron approximation, the wave functions fall into two categories. The first consists of localized or

bound states that decay exponentially with distance from the impurity. In the second, vastly more prevalent, category the orbitals resembles distorted band states that oscillate with increasing separation from the defect. Related matters are discussed further in Sec. III. It is a measure of the difficulty of this area that the range of occurrence of bound states in higher-valence solutes has not previously been identified experimentally or accurately predicted by calculation. It has, nevertheless, been widely believed among chemists that halide ions probably dissolve in alkali metals as ions with full p^6 valence shells bound below the host band edge.[4]

The nature of ionic effects for impurities in metals has also been largely neglected. To clarify the processes that make host-to-impurity charge-transfer processes of this type inevitable we consider the limit of a dilute monovalent solvent lattice with an exceedingly large lattice parameter a. The host valence states then fall in a narrow band near E_I in energy, with E_I the host-atom ionization potential. When an impurity with affinity $\mathcal{A}$ replaces one solvent atom there arises the possibility that the solid may find its state of lowest energy when one host electron is transferred to the impurity. The energy of the ionized configuration is least when the hole localizes near the impurity to screen the impurity charge; This involves an electrostatic energy $\sim -e^2/a$ for the tight-binding wave functions expected for large a (this is the case whether or not a lies beyond the Mott transition). Clearly, the ionic states lies lowest when

$$E_I - \mathcal{A} - e^2/a < 0. \tag{1}$$

For an alkali metal with $E_I \sim 4.5$ eV and a halogen impurity with $\mathcal{A} \sim 3.5$ eV, the ionization takes place for $a \sim 25$ a.u. Thus I with A = 3.3 eV, or Te with $\mathcal{A} = 3.6$ eV, is readily ionized, but Xe with $\mathcal{A} \sim -1$ eV is not. Note that for the case of a narrow host band and substantially favored ionicity, the valence orbitals of the ion are bound.

The possible occurrence of a second and further ionization steps is less easily analyzed because free multiply negative ions are universally unstable *in vacuo*, and multiple affinities derived from studies of salts pertain only to tightly bound orbitals. However, no principle forbids multiple ionizations; the ionicity of least energy prevails.

There are, nevertheless, subtleties related to the question of variable ionicity. Recent studies have identified excited states of certain impurity-metal complexes. In some cases the excited state has been created by optical excitation from the ground state, as in soft-x-ray absorption.[5] In other cases the excited states are thermally accessible and are present in thermal equilibrium at elevated temperatures. This happens for rare earths[6] and, perhaps, 3d transition-metal impurities also.[7] Two features of the observations bear special comment. First, the excited levels are quite sharp. For 100-eV core excitations the threshold is sharp to a few tenths of 1 eV, despite the enormous multiplicity of Auger-assisted recombination processes that are available.[5] Second, the excitation spectrum in several cases bears a surprising resemblance to the excitation spectrum of free impurity atoms (or ions), or to the spectrum of the solid wholly composed of impurity atoms.[6,8] Evidently there are features of the spectrum that an impurity atom may carry with it from one host to the next.[9] Since even an excited impurity remains neutral in a metallic solvent, the simplest excitations must resemble an electron and a hole lingering together at the impurity by virtue of their mutual attraction. The requirement of two particles makes clear the reason why Koopman's theorem becomes invalid and the local-excitation spectrum becomes insensitive to host properties. Indeed, detailed Hartree–Fock studies of core-hole excitation energies in metals, semiconductors, and alloys can reproduce to ~1% the observed edge energies.[10,11] What still remains unclear is the degree to which charge-transfer processes also conform to this scheme, so that impurity ionicities differing from the ground state may also be regarded as resonances in the excitation spectrum. Unfortunately, the studies reported in this paper are sensitive mainly to the ground state and shed only a limited light on the question of excited configurations. The main results pertain to the nature of the ground configuration.

The experimental results presented in this paper concern impurity magnetism in monovalent solvents. This proves particularly sensitive to the structural features exhibited by higher-valence impurities. An interpretation of these data and earlier beautiful results of Slichter and co-workers,[12] concerning the conduction-electron spin-flip scattering cross section of impurities, yields a deep insight into the broad structural trends of these interesting point defects.[1] A basic chemical understanding of lower-valence impurities has been available since the analysis by Odle and Flynn[13] of Knight shifts in solid and liquid alloys based on monovalent solvents. It hardly seems necessary to remark that these features reproduce essentially intact among solid and liquid alloys. The broad scheme has been further extended to deal with polyvalent metallic host lattices also.[14] Theoretical interpretations of the spin-flip data for monovalent solvents have conformed to the predicted trends.[15] However, as pointed out in preliminary reports,[1] these interpretations have overlooked the central chemical tendency of higher-valence impurities toward ionic configurations, often with bound va-

lence levels. When these effects are recognized, there emerges a coherent and occasionally quite detailed picture of the structure of positive-valence solutes in simple metallic solvents.

In what follows we first present, in Sec. II, a detailed experimental account of the susceptibility studies and then, in Sec. III, turn to an elucidation of the impurity structure.

II. EXPERIMENTAL DETAILS

Susceptibility measurements were made by the Faraday method using an inhomogeneous portion of the field provided by a 40 kG superconducting solenoid. A furnace housed inside the solenoid made available a working temperature range of 0–1150 °C that proved more than adequate for this work. The total field force of ~100 mg on a 1-cc sample with $\chi \sim 10^{-6}$ cm^3 was measured by means of a chemical balance and converted into an absolute susceptibility by subsidiary measurements on pure KBr and KCl. The calibration constant proved to be reproducible to about 1%, and this sets the systematic uncertainty in the susceptibilities reported below.

The materials studied contained either liquid-alkali-metal solvents or Ag-solvents in the liquid or solid state. Silver is an ideal, almost inert solvent that readily dissolves a wide variety of solutes. In contrast, the alkali metals present numerous difficulties, and the following account of sample preparation is mainly concerned with the problems encountered in dealing with these materials.

A. Sample Preparation

Alkali metals are, of course, hard to handle and become particularly reactive at elevated temperatures. Unfortunately, most desirable impurities dissolve appreciably in alkali metals only at high temperature in the liquid phase. The compromise between reactivity and the solubility required for this work was established in the temperature range 300–350 °C using fused quartz containing materials. With solubilities in many cases reaching 1–5% it was then possible to determine impurity susceptibilities with the necessary accuracy of $\pm 10^{-5}$ cm^3/mole (the order of magnitude of the host susceptibility) by means of susceptibility measurements having a precision of ~1%. This precision proved perfectly feasible for Na, K, Rb, and Cs (and, of course, the Ag solvents) in quartz in the stated temperature range, but we were quite unable to contain liquid Li in quartz even at substantially lower temperatures. For this reason we shall not report here any results for Li solvents.

According to the manufacturer's claims, the alkali metals employed in this work had a purity of 99.9+%. Somewhat more pure samples of Na and K were also obtained and employed upon occasion. The Ag, and all solute elements used in alloy fabrication, were of stated 99.999% or higher purity.

All manipulations of the alkali metals were conducted in a glove box filled with dry Ar. The materials were shipped under oil and transferred during use into dry ether, to wash off residual oil, and to protect the metal surface from attack by residual oxygen or water vapor. Small admixtures of ethanol into the ether provided a well-controlled etching solution with which surface contaminants could be eliminated. Great care is required to maintain the more reactive alkali metals clean and pure. For those cases for which an alkali-metal alloy was required as a host material for impurities, a master alloy was first prepared and allowed to homogenize in the liquid phase under ether for several hours. Portions required for individual alloys could be extracted very satisfactorily by means of a pipette.

The susceptibilities reported in this paper were obtained using a type of sealed and evacuated specimen capsule similar to that designed by Peters.[16] The capsules are described below. Weighed quantities of the host and impurity metals were placed into calibrated capsules filled with dry Ar. The capsules were then evacuated and sealed off. No deliberate effort was made to alloy the metals before undertaking the susceptibility runs. Any mixing caused by heating prior to the run would inevitably be reversed by subsequent precipitation when cool; therefore, the time lapse at high temperature was minimized by alloying the metals inside the susceptibility furnace during the run. It normally required from 1–3 h at the test temperature before the susceptibility stabilized. In several doubtful cases for which existing phase diagrams[17] are inadequate the solubility was investigated by etching rapidly cooled alloys to determine whether or not the initial piece of solute material had become dispersed. The solubilities of Ag and of NaI in Na both proved too small for useful susceptibility measurements. Problems also arose owing to the explosive speed with which Se and Te dissolve in K; K_2Se and K_2Te were employed as impurities instead. Difficulties of a different nature that arose for NaK-host alloys are described in Sec. II B.

We found that the efficacy of the procedures employed to obtain clean specimens improved markedly with practice. Occasional signs of oil contamination did appear in the capsules and, in some cases, patches of tarnish are evident at the metal-quartz interface. However, many samples have maintained mirror surfaces for two years after use in high-temperature measurements.

A sketch of the capsules employed in this work

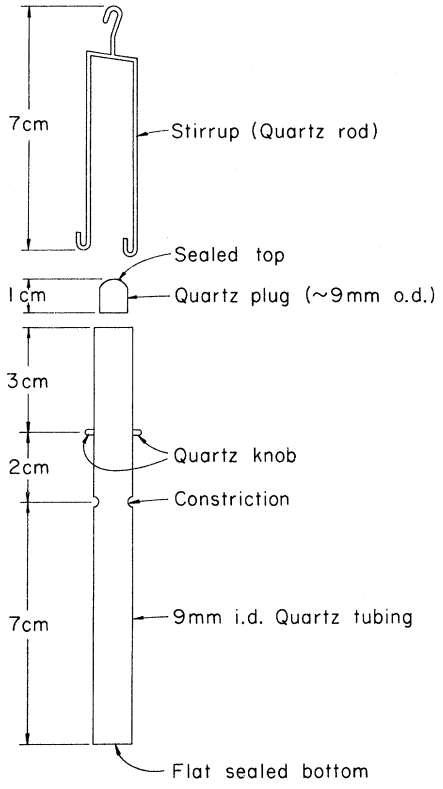

FIG. 1. Sketch of the quartz specimen holders used in the measurement of susceptibilities for liquid alloys. Each sample required a separate holder, which was calibrated prior to use.

is given in Fig. 1. Capsules must be nonreactive, with a small temperature-insensitive susceptibility; they need to be short, in order that vapors are confined in a region of uniform temperature, and must be sealed under vacuum to isolate the sample from fresh contaminants. Those transition metals suitable for containing molten alkali metals fail to satisfy the susceptibility requirements and are difficult to seal under suitable conditions. Quartz therefore emerges as a desirable choice. However, as there appears no way in which one capsule can be used for many samples, each specimen has to be sealed into its own, previously calibrated, capsule.

The capsules finally chosen hang freely from a quartz stirrup. They are fashioned from 11-mm-i.d. quartz tubes, having 1-mm walls and selected for uniformity. After a susceptibility calibration run at the test temperature, the cool capsules were flushed with Ar, loaded with metal, evacuated, and the 9-mm-diam quartz stoppers fused into position at the constriction. This procedure left the susceptibility calibration unchanged because the length remained constant and because the fused region fell well outside the volume of strong field gradient. A minor correction (~ 3 mg) was required to eliminate the change of buoyant force caused by vacuum encapsulation. In addition, a correction of typically ~ 2% was needed to allow for the variation of calibration constant over the sample length of ~ 2 cm.

B. Results

For convenience in what follows we divide the results into data pertaining (i) to detailed results for Na- and K-based solutions, (ii) to the variation of susceptibility with host properties for certain particular impurities, and (iii) to the unusual properties of Ag-band solutions.

(i) *Impurities in liquid* Na *and* K. In order to increase the accuracy with which the molar impurity susceptibility could be determined in a particular host lattice, from three to six alloys of varying composition were studied. With a few exceptions, notably for Ag (see Sec. IIA) and Sn in NaK solvents (see what follows), the molar alloy susceptibility $\chi(c)$ proved to vary linearly with impurity content c(at.%). The results were therefore analyzed using the expression

$$\chi(c) = c\chi_i + (1-c)\chi_h, \tag{2}$$

with χ_h the molar susceptibility of the host lattice. Some typical results for impurities in liquid Na and liquid K at about 320 °C are given in Figs. 2 and 3.

Values of the solvent susceptibilities were also obtained during the course of these studies. In the case of liquid Na we obtain an apparently trustworthy result

$$\chi_{Na} = (16.1 \pm 0.3) \times 10^{-6} \text{ cm}^3/\text{mole}.$$

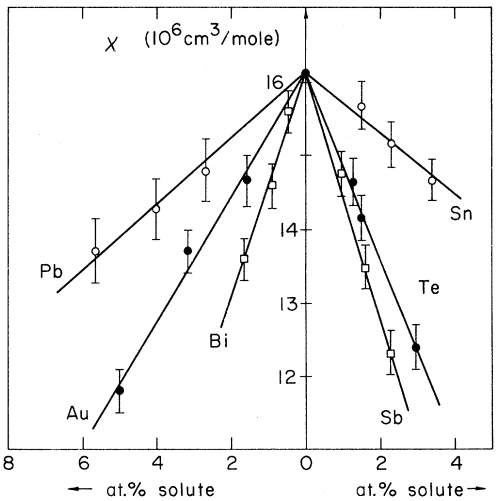

FIG. 2. Susceptibilities of some liquid-Na-based alloys containing Sn, Sb, Te, Au, Pb, and Bi, shown as functions of impurity concentration.

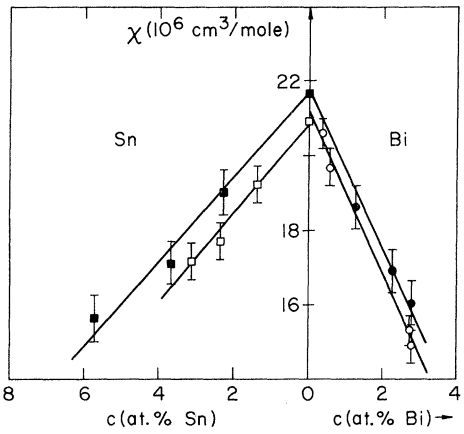

FIG. 3. Susceptibilities for some liquid-K-based alloys containing Sn and Bi, shown as functions of impurity concentration. Two sets of data using different batches of K are shown for each impurity. The differences in the susceptibilities of the unalloyed batches of K do not seem to affect the impurity susceptibilities, which depend on the slopes of the lines drawn through the points.

This is in excellent agreement with the value 16.1×10^{-6} cm^3/mole reported by Bowers,[18] but disagrees with the result 14×10^{-6} cm^3/mole given by Collings.[19] The random error among ten results was only $\pm 0.06 \times 10^{-6}$ cm^3/mole, and the uncertainly cited is thought to be generous. No such confidence can be expressed in the result for liquid K. Different batches were found to vary in susceptibility by up to $\pm 10^{-6}$ cm^3/mole depending on exposure to oil and, perhaps, other variables. Careful measurements on a purer (99.99%) grade of K fresh from a sealed capsule containing no oil yielded

$$\chi_K = 21.7 \pm 0.4 \times 10^{-6} \text{ cm}^3/\text{mole}.$$

Fresh 99.9% K yielded an identical result as a mean of five samples, among which the rms scatter was again only $\pm 0.06 \times 10^{-6}$ cm^3/mole, but the degree to which this value is influenced by residual contaminants remains obscure. The susceptibility of higher potassium oxides is enormous ($\chi = 3230 \times 10^{-6}$ cm^3/mole for KO_2). However, this uncertainty for the pure materials has little influence on the accuracy of the impurity susceptibilities deduced for alloys. As illustrated by the cases of Bi and Sn, shown in Fig. 3, the change of χ with impurity concentration is sensibly independent of the particular host material employed.

Impurity susceptibilities in the Na solvent were obtained from straight lines drawn through the alloy data with $\chi = 16.1 \times 10^{-6}$ cm^3/mole at $c = 0$. A similar procedure was employed with $\chi = 21.7 \times 10^{-6}$ cm^3/mole for the six K alloys fabricated from the purest K material. Other K alloys were analyzed using the best straight line through the set of data. This procedure is appropriate because all alloys of an impurity were made together from a common solvent batch and run successively as a group.

Values of the impurity susceptibilities determined in this way for twenty solutes are presented in Table I. Particularly striking is the appearance of a giant diamagnetism[1] for pnictide and chalcogenide impurities in both Na and K. The case of Sn, for which an incipient diamagnetism is apparent in the K solvent, is discussed in (ii).

(ii) Rb, Cs, *and* NaK-*alloy solvents*. The results collected in Table I show systematic trends of diamagnetism with impurity valence. In addition, certain impurities exhibit large changes of diamagnetism between solvents. This is notably the case for Sn and, to a lesser extent, Bi, for which χ decreases substantially in passing from K to Na. For this reason we have investigated the susceptibility of Sn as a function of (monovalent) host-electron density by use of Cs, Rb, NaK-alloy and liquid-Ag solvents.

Liquid Rb and Cs solvents present difficulties similar to those described above for K, and no unique values for the host susceptibilities were established; the remaining pure solvent, Ag, is discussed in (iii). In the case of NaK alloys we have determined the alloy susceptibility as a function of composition across the entire phase diagram. These results have been systematically corrected for the use of the less pure grade of K (the correction amounts at most to several percent), and the results may be somewhat less reliable than their excellent internal consistency. They show that the susceptibility of NaK alloys sags slightly below the linear interpolation between the results for pure Na and pure K (Fig. 4). Similar, but less precise, data are available for other molten alkali-metal alloys.[20]

The molar susceptibilities of Sn in the various solvents were obtained from five or six alloys of

TABLE I. Molar susceptibilities (-10^{-6} cm^3/mole) of impurities in liquid Na and liquid K at 300 °C.

Impurity	Solvent Na	Solvent K
Se	...	113 ± 17
Cd	18 ± 5	...
In	5 ± 10	53 ± 12
Sn	26 ± 8	98 ± 8
Sb	148 ± 15	154 ± 13
Te	108 ± 14	112 ± 30
Au	69 ± 8	82 ± 5
Hg	29 ± 8	37 ± 10
Tl	10 ± 8	25 ± 10
Pb	29 ± 9	28 ± 15
Bi	136 ± 14	202 ± 15

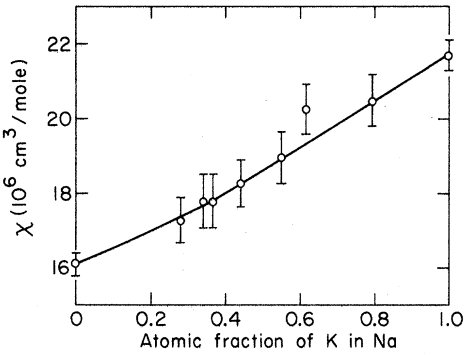

FIG. 4. Susceptibility of liquid-NaK alloys at $T \simeq 320\,^{\circ}C$. Data taken on alloys made from impure K have been corrected to conform with the susceptibility of the K end point taken from several samples of the purest K. The correction is at most ~3%.

varying Sn composition based on each host metal or master alloy. In the case of NaK alloys a difficulty arose that was eventually assigned to limited Sn solubility. Initial runs were conducted with four alloys for each solvent and impurity concentrations of up to almost 4-at.% Sn. These led to best line fits that exhibited a peculiar hump near the transition of χ_{Sn} as a function of host-electron density. Because χ_{Sn} is only of moderate size in this range, and owing to the difficulties mentioned above for K solvents, any accurate resolution of the susceptibility transition lies very close to the limits of our available experimental precision. A determined effort, using six fresh Sn alloys with $c < 2\%$ for each master NaK alloy, eliminated the problem and gave the final data displayed in Fig. 5. It therefore appears that the Sn solubility is limited in the alloy solvents, although the available time and accuracy were insufficient to estimate details of the solubility and its dependence on host composition.

The Sn-impurity susceptibility seems to vary systematically with host-electron density n_e. Figure 5 shows that χ_{Sn} undergoes a fourfold decrease between $n_e = 100$ and $n_e = 200$ electrons/Å^3, and thereafter becomes remarkably stable. A more abrupt transition is indicated by the dotted line also passing through the points; the data are sufficiently uncertain to accommodate either of these alternatives. Sketched into Fig. 5 as broken lines are similar trends that may describe analogous transitions of In, Sb, and Te impurities. Additional data concerning these solutes in liquid Ag [see (iii)] and other solvents, included in Fig. 5, establish the existence and approximate location of the Sb and Te transitions. The precise positions of the transitions could not, however, be determined owing to the difficulty of containing Li-based alloys. Figure 6 shows similar, but even more sparse, data for Au and Bi.

(iii) *Impurities in liquid and solid* Ag. In many ways the results for Ag-based alloys were the most surprising encountered in this work. Earlier extensive and systematic studies of solid Ag- and Cu-based solutions by Henry and Rogers[21] reveal a large impurity diamagnetism that increases almost linearly with solute valence up to $\sim -10^{-4}$ cm^3/mole for Sb or As. These results were verified

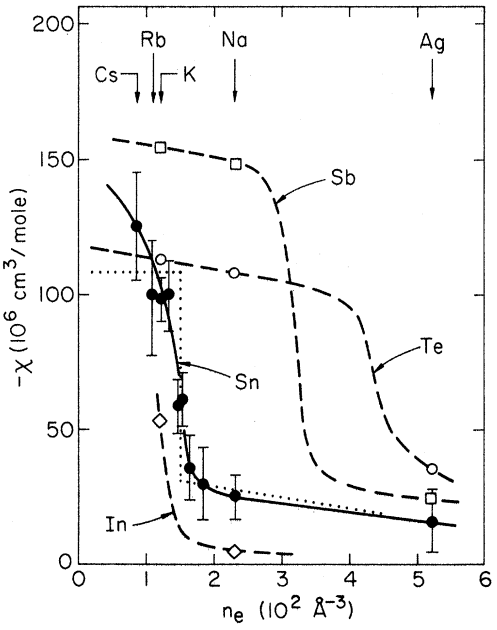

FIG. 5. Susceptibility of some Ag-row impurities as a function of (approximate) host-electron density, in monovalent liquid solvents. The solid and dotted lines indicate possible forms of the transition of χ for Sn impurities. The broken lines represent systematic guesses at the forms of analogous transitions for In, Sb, and Te, fitted to the available data.

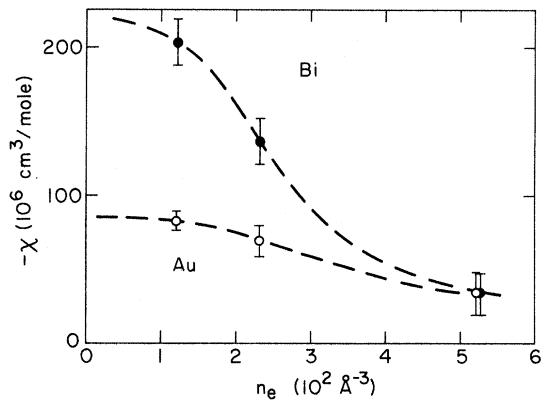

FIG. 6. Susceptibility of Au and Bi as a function of host-electron density in liquid monovalent solvents. Broken lines suggest possible forms for the transitions.

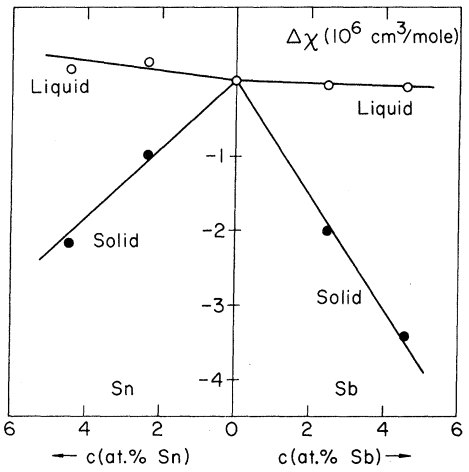

FIG. 7. Changes $\Delta\chi$ of the susceptibility, shown for Ag-based solid alloys (full circles) and liquid-Ag alloys (open circles) as functions of the Sb and Sn concentrations. The large impurity diamagnetism of the solid alloys is reduced and becomes insensitive to the solute species upon liquification.

in part during the present work and extended to liquid alloys also.

Measurements were undertaken in the solid phase at room temperature and in the liquid phase at 1000 °C using methods similar to those discussed above for alkali-metal solutions. For liquid Ag at 1000 °C we obtained

$$\chi_{Ag} = (-22.4 \pm 0.4) \times 10^{-6} \text{ cm}^3/\text{mole}$$

and for the solid

$$\chi_{Ag} = (-19.1 \pm 0.4) \times 10^{-6} \text{ cm}^3/\text{mole} .$$

The latter result is to be compared with the value -19.56×10^{-6} cm^3/mole reported by Henry and Rogers.

The alloys studied at room temperature contained Sn or Sb impurities. They were annealed for two days at 550 °C in the solid phase and quenched to room temperature before use; this conforms to the procedures of Henry and Rogers. Figure 7 shows as open points the changes in molar alloy susceptibility as a function of impurity concentration. Also shown in Fig. 7 are the changes in molar susceptibility with impurity concentration of *liquid*-Ag alloys containing Sn and Sb. The results for liquids are strikingly different from those for the solid. There is no doubt whatever that the anomalously large and valence-sensitive diamagnetism disappears in the liquid phase. For the case of one Ag alloy containing 6-at.% Cu, Henry and Rogers present results for $T = 700$ °C suggesting that the impurity magnetism is insensitive to temperature in the solid phase. We have verified that the susceptibility of Sb in Ag is similarly insensitive to temperature up to 700 °C. It appears, therefore, that the major change of impurity magnetism takes place at the melting transition.

Impurity susceptibilities for eight impurities in liquid Ag, and for the two impurities in solid Ag, are collected in Table II. Also tabulated are the room-temperature results of Henry and Rogers. The two sets of data for solid alloys are in excellent agreement. However, the large, linear valence dependence of susceptibility observed for the solid alloys gives way to a smaller and almost featureless diamagnetism in the liquid. The results are also in striking contrast with those reported above for liquid alloys based on Na and K solvents. The valence dependence of the impurity susceptibilities in K, Na, and Ag liquid solvents are contrasted in Fig. 8 for Ag-row impurities and in Fig. 9 for Au-row impurities.

TABLE II. Molar susceptibilities (-10^{-6} cm^3/mole) of impurities in liquid Ag at 1000 °C and solid Ag at 20 °C. HR indicates results of Henry and Rogers (Ref. 21), P marks the present results.

Impurity	Ag	Sn	Sb	Te
liquid (P)	22.4 ± 0.4	16 ± 11	24 ± 9	36 ± 7
solid (P)	19.1 ± 0.4	66 ± 10	96 ± 10	...
solid (HR)	19.56	74	100	...

Impurity	Au	Hg	Tl	Pb	Bi
liquid (P)	33 ± 12	34 ± 13	22 ± 13	33 ± 13	33 ± 13

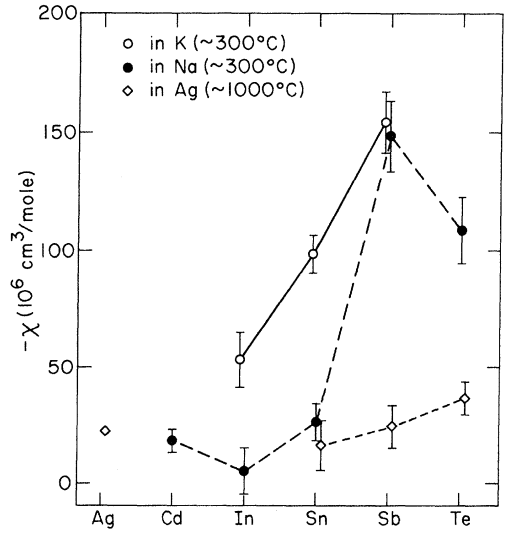

FIG. 8. Variation of impurity susceptibility with solute valence for Ag-row impurities in liquid alloys based on K, Na, and Ag.

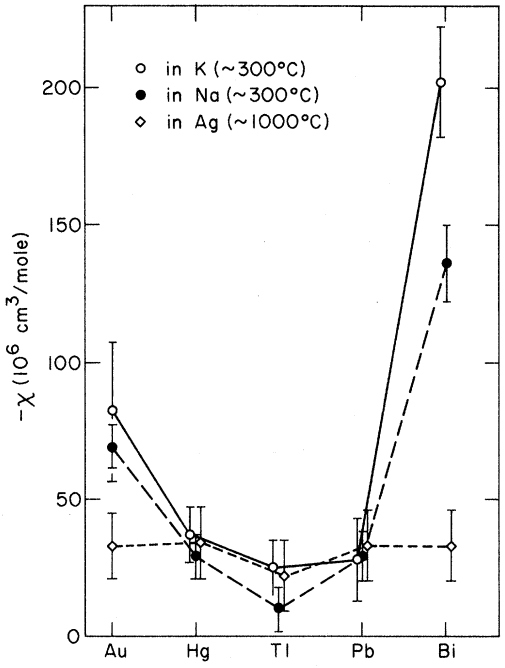

FIG. 9. Variation of impurity susceptibility with solute valence for Au-row impurities in liquid alloys based on K, Na, and Ag.

III. DISCUSSION

Several comprehensive discussions of impurity magnetism have been published,[22] but applications of the results to particular impurities have not provided a successful account of the observed susceptibilities. It seems unlikely that the general theory presented by Kohn and Luming[23] is incorrect for the free-electron solvents visualized in their work. Rather, the discrepancies probably arise from the impurity structures assumed in specific calculations and from deviations of the host materials from the idealized free-electron model. The latter point gains in significance from the strikingly dissimilar results presented here for liquid- and solid-Ag-based alloys; we shall see that these effects point rather clearly to the influence of a complex host band structure. However, for the liquid-alkali-metal solvents of interest here, and perhaps for liquid Ag also, no such sharp structural effects can be anticipated. For this reason our theoretical discussion can rest with reasonable surety on the theory laid down in previous work, and will focus mainly on the topic of impurity structure, to which we now turn.

We recall first that the one-electron functions of the host lattice in the presence of the impurity are specified by phase shifts η.[24] These determine the particular combination of two degenerate orbitals of the perfect lattice, one finite and the other diverging at the impurity site, that gives the correct wave function outside the impurity in the imperfect lattice. This wave function matches smoothly onto the impurity wave function in the defect cell. A simplified free-electron scheme and eigenfunctions of angular momentum are often employed in a partial-wave analysis of this type, but alternative functions having a symmetry better suited to the host lattice could be used instead. For the present purposes the simple scheme will suffice and we shall use eigenfunctions of angular momentum specified by quantum numbers of wave vector k (or energy E), spin s, and orbital angular momentum l and its projection m along a chosen axis. The orbitals are then fixed in Hartree–Fock theory by phase shifts $\eta_{lms}(E)$. Only in a restricted theory are the oribitals for given E and l necessarily degenerate.

The impurity structure is then defined[3] in terms of the phase shifts by the density of *excess* impurity states for those quantum numbers:

$$N_{lms}(E)=\frac{1}{\pi}\frac{d\eta_{lms}}{dE}. \tag{3}$$

This equation is closely related to the expression

$$\tau_{lms}=2\hbar\frac{d\eta_{lms}}{dE} \tag{4}$$

for the time an electron lingers near the impurity, and to the Friedel sum rule[25]

$$z(E_F)=\sum z_{lms}=\frac{1}{\pi}\sum_s\sum_{lm}\eta_{lms}(E_F) \tag{5}$$

giving the total excess charge located near the defect. The number of electrons localized in states bound below the band bottom at $E=0$ is

$$z(0)=\frac{1}{\pi}\sum_s\sum_{lm}\eta_{lms}(0). \tag{6}$$

We shall offer some preliminary comments concerning bound and nonbound states since this distinction plays an important part in what follows. In one-electron theory, bound orbitals decay exponentially at large distances from the defect while unbound states oscillate like band states. Typical variations of phase shifts as a function of energy, and impurity densities of states, are shown for the two cases in Fig. 10. Four patterns of phase shifts and excess state densities, corresponding, respectively, to bound levels, virtual levels, resonance levels, and band states, are indicated in the figure.

It has been pointed out by Odle and Flynn[13] that impurities in metals suffer the loose chemical constraint that the ground-state screening-charge distribution in the impurity and solvent cells must be distributed among angular momentum components

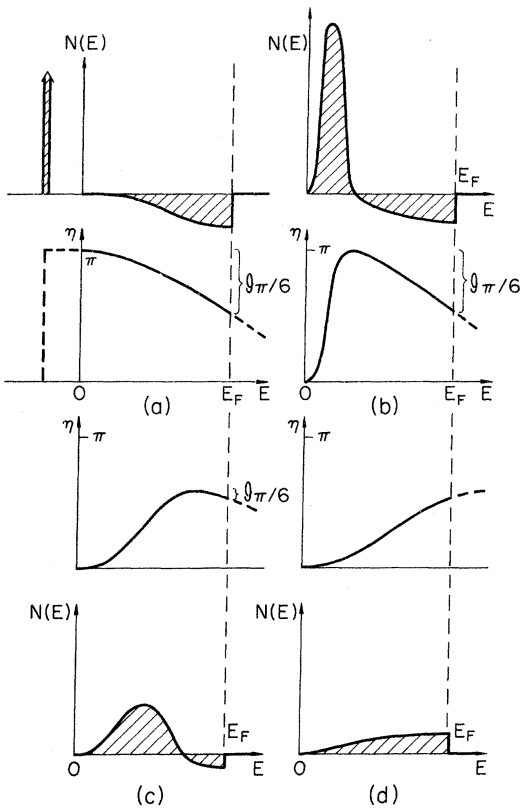

FIG. 10. Some patterns of phase shifts η sketched as functions of electron energy between $E=0$ and $E=E_F$. Also shown are the densities of excess impurity states $N(E)=\pi^{-1}(d\eta/dE)$. It is important in the present studies that $N(E)$ is *negative* at E_F for (a) bound states, (b) virtual bound states , and (c) resonant levels, but not for the band states shown in (d). The ionicity g, according to Eq. (7) for the case of p waves, is shown in (a), (b), and (c). It is the area of the negative portion of $N(E)$.

roughly as in free atoms. For a given impurity in a specific host the phase shifts at E_F, being related by Eq. (5) to the components z_{lms} of the screening charge, are therefore fixed approximately by free-atom structures. This principle appears to find its justification in both experimental studies[13] and in detailed theoretical calculations.[12] The four cases shown in Fig. 10 obey this constraint, and the different patterns lead to separate impurity structures. It is our belief that the distinctions among these structures are of great importance in determining properties, such as spin-flip scattering and impurity susceptibility, that are influenced by the distribution of screening charge as a function of electron energy.

A. Ionicity

The phenomenon of ionicity introduced in Sec. I finds its natural expression in terms of phase shifts. To simplify the discussion we shall restrict attention to the p-wave phenomena of central concern for the impurities in monovalent hosts of interest here. It will become apparent that the higher-valence impurities must each bind two s states near or below the band bottom, and experimental indication of this trend have previously been reported by Harrison[26] for Si impurities, even in the relatively broad conduction band of Cu. Since the host bands are s-like with one electron per cell, the s-wave phase shift must fall off from π to $\sim\pi/2$ between $E=0$ and $E=E_F$, in accordance with the proposal of Odle and Flynn. The screen then contains approximately one excess s-like state (two being bound and one repelled in the band) and the remaining excess screen is largely p-like. An impurity with Z valence electrons, two s-like and $Z-2$ p-like, thus has $\eta_1(E_F)=(Z-2)\pi/6$ (provided the orbitals are degenerate at E_F). The remaining structural features of interest here then relate to the variation of η_1 with E through the band, together with any details of bound p states.

We shall call the *fully ionized* configuration of a higher-valence impurity that state in which a full shell of p electrons is localized at the defect in states near or below the band bottom. When the states are bound, this is indeed the fully charged ion in the chemical sense; it is neutralized in the metal by repelled band states that form a hole in the electron gas, and hence provide a Madelung well to help bind the ion. But, since a precise distinction between bound and low-lying virtual states exists only in the one-electron approximation, we may conveniently regard the latter as ionic also. Thus, both the bound and virtual patterns of η in Fig. 10 are for all practical purposes fully ionic. We see than that the decrease of the phase shift from its maximum to E_F provides a useful and quantitative definition of ionicity that is appropriately insensitive to the detailed behavior near $E=0$. The negative charge bound on the ion at low energies is

$$g=\frac{6}{\pi}\,[\bar{\eta}_{\max}-\bar{\eta}(E_F)], \tag{7}$$

in which the $\bar{\eta}$ represent average p-wave phase shifts of the several orbitals. This definition coincides with $8-Z$ for fully ionized impurities, and provides a useful measure of p-wave ionicity for virtual and resonant states.

Greater complexity and unresolved problems are met when the orbitals are not degenerate, and when the impurity is less than completely ionized. There appears no reason why an incomplete shell of electrons cannot be bound below the conduction-band bottom. Consider, for example, the atomic configuration of a halogen impurity having two bound s states and five bound p states. Two pat-

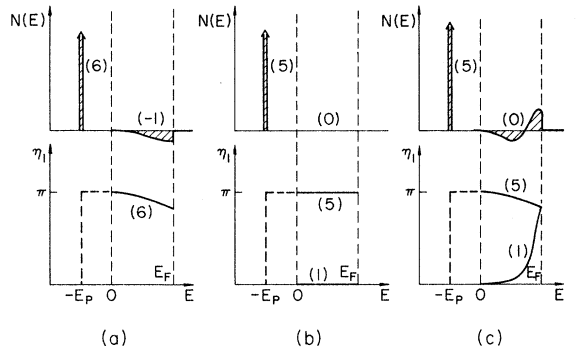

FIG. 11. (a) Structure of the I^- ion and (b) and (c) two possible structures of the neutral I atom in monovalent metals. The numbers in parentheses in the sketches showing $N(E)$ give the areas under the curves, and those in the sketches showing η give the number of degenerate phase shifts. E_p is the binding energy of occupied p orbitals.

terns of nondegenerate p-wave phase shifts are given in Figs. 11(b) and 11(c). The configuration in Fig. 11(c) has five degenerate phase shifts similar to the six that occur for the fully ionized halogen (e.g., I^-), and one orbital that replaces bound-state screening by band screening. The alternative p states have equal total occupancies, but do not all bind electrons at the same mean energies. Figure 11(b) shows the opposite limit in which one orbital remains completely unoccupied. A wide variety of intermediate cases can also be visualized.

Configurations (b) and (c) are, in principle, acceptable alternatives to the ionic halogen configuration (a) although, as we shall see, they can probably be ruled out in practical cases. The empty orbital in Fig. 11(b) is maintained by Coulomb correlations if the energy required to eliminate the screen and place an electron in the empty p orbital happens to be positive. These structures are potentially magnetic owing to the differently occupied orbitals, and may cause strong spin-flip scattering; they are, in fact, examples for the Anderson model[27] of impurity magnetism. A difficulty arises in that the five other configurations having alternative orbitals differing from the remainder are degenerate with that shown, and interactions with the conduction electrons can then take the impurity from one configuration to the next in a way that finds no useful representation on the Hartree–Fock model. The frustrating problems that follow have been studied in many theoretical attacks on the Kondo effect.[28]

Difficulties of this type do not occur when the orbitals of the *fully* ionic configuration are split instead by spin-orbit coupling in the impurity core or by crystal fields. Linear combinations of the orbitals then fall into sets of states with new degeneracies, and the behavior of these new, fully occupied sets of degenerate levels may be treated as outlined above for s and p states. With a *partial* occupancy of any set, however, one returns to the former difficulty. Phase shifts are shown schematically in Fig. 12 for $l=1$ and $j=\frac{3}{2}$ and $\frac{1}{2}$ for several spin-orbit-split configurations having only degenerate levels. In each case the splitting between $\eta_{3/2}$ and $\eta_{1/2}$ is small when $d\eta/dE$ is small or negative. This seems appropriate because the associated small or negative density of impurity states localized near the solute atom ensures that host-band electrons rarely experience the spin-orbit interaction in the impurity core. We shall see in what follows that this has an important bearing on the interpretation of the observed impurity spin-flip scattering cross sections in alkali-metal hosts.

B. Interpretation of Susceptibility and Spin-Flip Scattering Results

Figures 13 and 14 show for Ag-row and Au-row impurities in Na the impurity spin-flip scattering

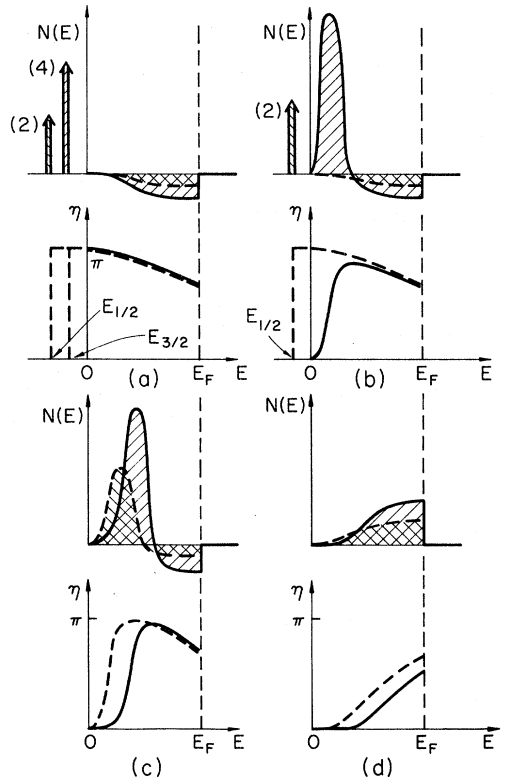

FIG. 12. Effect of spin-orbit splitting on the phase shifts of alternative structures of Te in monovalent metals. The p-wave phase shift with $j=\frac{1}{2}$ is indicated by a broken line and that for $j=\frac{3}{2}$ is shown by the solid line. A similar convention is used to distinguish the densities of states $N(E)$ with $j=\frac{1}{2}$ and $j=\frac{3}{2}$.

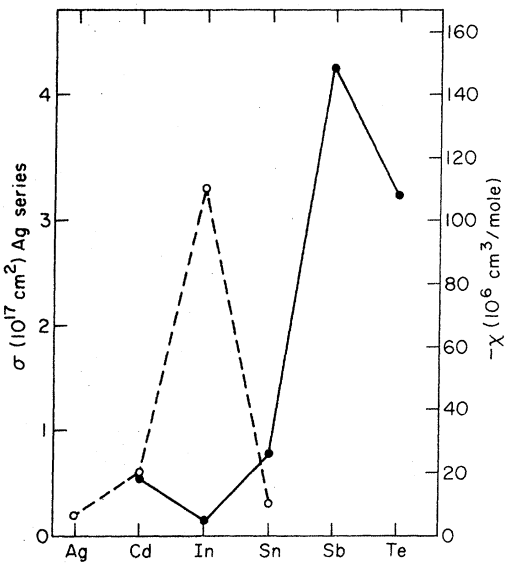

FIG. 13. Molar susceptibility χ and the spin-flip scattering cross section σ of Ag-row impurities in Na. The emergence of resonant or bound $5p$ levels is indicated by the way σ decreases abruptly and χ becomes strongly negative for Sb and Te impurities.

cross sections published earlier by Slichter *et al.* and the impurity susceptibilities reported here. Similar results are available for spin-flip scattering in the Li-host lattice and for susceptibilities in K (see Sec. III A), but no other data show the two trends in a common solvent. The striking qualitative feature that emerges from this comparison is that the onset of giant diamagnetism with increasing valence at $Z \sim 5$ is accompanied by the remarkable decrease in σ_{SF} reported by Asik, Ball, and Slichter.[12] Our interpretation of these results is that the impurity p orbitals, which occur as band states for $Z \leq 3$, gradually fall and sharpen into degenerate virtual levels for $Z \sim 5$ and finally emerge below the band bottom as fully bound orbitals for $Z \simeq 6$, 7, and 8. The boundaries among these domains are diffuse and certainly depend to some extent on details other than the impurity valence alone.

Consider first the spin-flip scattering. Asik, Ball, and Slichter show that, to the neglect of d-wave and higher-order scattering,

$$\sigma_{SF} \propto \sin^2[\eta_{3/2}(E_F) - \eta_{1/2}(E_F)] \tag{8}$$

depends only on the difference between the $j = \frac{1}{2}$ and $\frac{3}{2}$ p-wave phase shifts at E_F. Following Cornell and Slichter[12] we write for the case of weak spin-orbit coupling

$$\eta_{3/2}(E) - \eta_{1/2}(E) = \lambda(Z, E)\frac{d\eta_1}{dE}, \tag{9}$$

with $\lambda(Z, E)$ a spin-orbit splitting that has some energy dependence and η_1 the p-wave phase shift for $\lambda = 0$. From Eq. (3) we find

$$\sigma_{SF} \propto \lambda^2(Z, E_F)N^2(E_F). \tag{10}$$

Now λ is presumably comparable with the atomic spin-orbit splitting and varies only slowly with energy. Since λ increases monotonically through any row of the Periodic Table we see that the decrease of σ_{SF} by an order or more in magnitude for $Z > 3$ can only be ascribed to a radical decrease in the impurity density of states at E_F. Since the total p-wave screen must be preserved, for reasons outlined above, we conclude that the striking variation of σ_{SF} with Z can only be ascribed to the fact that the p-wave screening orbitals fall almost entirely below E_F. The results provide unambiguous evidence that resonant, virtual, or bound levels form.

A precise, nonperturbative description, including the energy dependence of λ is provided by the correct phase shifts. The sequence of model phase shifts for band, resonant, and virtual impurity orbitals given in Fig. 12 gives a qualitative account of the transition in σ_{SF}.

Let us now turn to the susceptibility results. Flynn and Lipari,[1] following Kohn and Luming,[23] analyze the impurity susceptibility into three terms. The first

$$\chi_p = \mu_B^2 \sum_r N_r(E_F) \tag{11}$$

gives the change in host spin paramagnetism, with

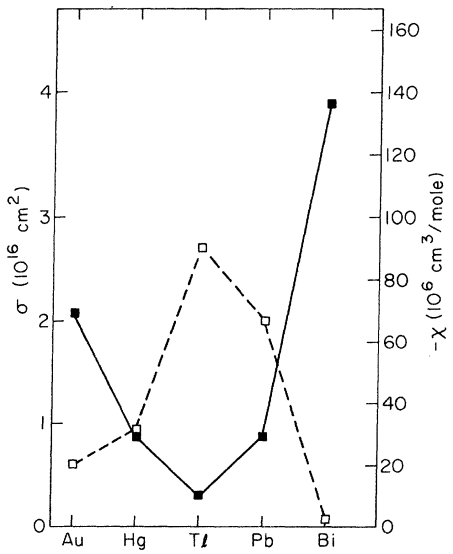

FIG. 14. Molar susceptibility χ and the spin-flip scattering cross section σ of Au-row impurities in Na. The emergence of resonant $6p$ levels is indicated by the way σ decreases and χ becomes strongly negative for Bi impurities.

TABLE III. Comparison between the experimental impurity susceptibilities reported here (expt.) and the predictions (theor.) of Flynn and Lipari (Ref. 1) for the fully ionic model of impurity structure. Values are given in -10^{-6} cm^3/mole.

	in liquid Na		in liquid K	
	expt.	theor.	expt.	theor.
Se	...	...	113 ±17	107
Sb	148 ±15	157	154 ±13	188
Te	108 ±14	108	112 ±30	125
Bi	136 ±14	168	202 ±20	198

r the quantum number that defines the impurity phase shifts. The second term describes orbital diamagnetism. For the bound core orbitals to which we confine attention here the contribution χ_c is identical with the expression used for free atoms. There remains a small orbital paramagnetism from perturbed band states which, together with a term that corrects the theoretical expressions to partial molar quantities, sum to a small, final correction, χ_d. This term has no important structure dependence and will be ignored in most of what follows.

χ_p and χ_c each make important contributions to the observed giant diamagnetism of higher-valence impurities. As the p orbitals fall below E_F with increasing Z, and the impurity densities of states becomes negative, the density of states near E_F and the host spin magnetism are both sharply reduced. Further, when the p orbitals fall to the band bottom and below they spread, being weakly bound, and the large $\langle r^2 \rangle$ of the orbitals is reflected in a large core diamagnetism. Thus, the susceptibility results find their explanation in precisely those structural trends deduced above from σ_{SF}.

A detailed theoretical study of the giant diamagnetism has been made by Flynn and Lipari.[1] They calculate by Hartree–Fock methods core orbitals that are consistent with the electron-gas response, and so obtain χ_c. They also show that for model phase shifts appropriate for fully ionic configurations of total ionicity g,

$$\chi_p = -(g + \tfrac{1}{3})\chi_e \quad (g \geq 0), \tag{12}$$

with χ_e the paramagnetic part of the host electron-gas susceptibility. The impurity susceptibilities obtained in their analysis are compared in Table III with the experimental results reported here. The substantial success met by the predictions for pnictide and chalcogenide impurities from this ionic model suggests that for $Z = 6$ the fully ionic model is valid. This indication is born out by other evidence discussed in Sec. III C. We note finally that the observed susceptibility of I^- in salts,[29] if corrected for metallic host paramagnetism, fits well into the sequence of impurity susceptibilities reported here.

C. Susceptibility Transition and Related Results

Figure 5 above shows the susceptibility of Sn impurities as a function of the electron density n_e of the host lattice in various liquid solvents. Similar, less detailed, results are also given for In, Sb, and Te. These results will be used here to identify the position of the impurity p levels with respect to the conduction band.

Consider first the nature of the Sn results in comparison to the data for Sb and Te. For fully ionic configurations the diamagnetism must increase with decreasing Z because the density of impurity states becomes progressively more negative in order to preserve the screening condition $\eta_1 = (Z - 2)\pi/6$ at E_F. The observations for Sb and Te, and the prediction for I, conform to this important trend, but even in those solvents with small n_e the Sn susceptibility of $\sim -125 \times 10^{-6}$ cm^3/mole falls well below the Sb result of ~ -170 cm^3/mole. This constitutes a *certain* indication that the observed Sn transition is *not* related to the transition from bound to virtual states in a fully ionic impurity. Nevertheless, the small spin-flip scattering cross section in Li and Na, together with the incipient magnetism, indicate that the p-wave phase-shift derivative at E_F is small or negative. Therefore the evidence points unambiguously to the development of a p-wave resonance (we shall discount the unlikely possibility that Sn adopt a partly ionic configuration with some bound p orbitals).

Sb and Te exhibit correct relative susceptibilities that also conform closely to the predicted theoretical magnitudes. This is strong evidence that the structures do bear a close resemblance to the fully ionic model. However, some care is needed because, even in one-electron theory, the susceptibility changes smoothly as bound states emerge. This point is established by Kohn and Majumdar.[30] When the exact wave function is considered,[31] the one-electron levels, and their relation to one-electron band levels, lose all precise meaning and it is to be expected that the transition from bound to virtual levels is accompanied by a smooth and, perhaps, rather broad maximum in diamagnetism. There appears a marked tendency in the cases of Sb and Bi for the predictions in Table III to be somewhat larger than the observed susceptibilities, and this may well mean that the full p levels of these impurities lie near the host band edge.

Further evidence comes from the values of n_e at which the susceptibility transitions in Fig. 5 occur. Since the conduction bands studied are 2–5 eV wide one may reasonably estimate that the

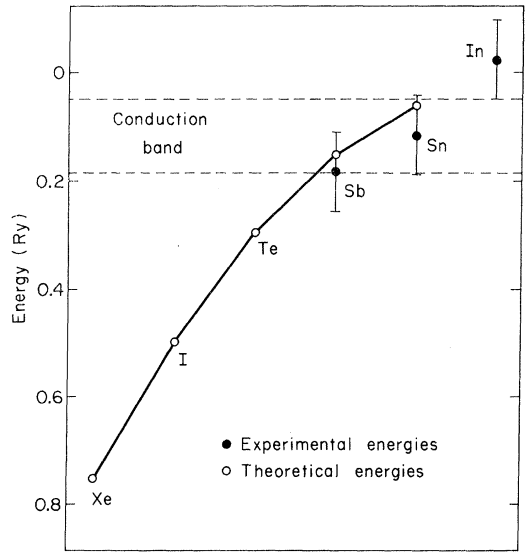

FIG. 15. One-electron energies for $5p$ orbitals of some Ag-row impurities in K, as deduced in the text (solid circles) and as calculated by Flynn and Lipari (open circles). An estimated exchange energy of ~0.18 Ry and a bandwidth of ~0.13 Ry have been used to draw in the conduction band. Correlation is neglected for both bound and band orbitals. The theoretical estimates are more reliable for deep levels.

Sn transition lowers the p levels by at least ~1 eV, from above E_F, with $d\eta/dE$ positive, to below E_F, with $d\eta/dE$ negative. But the Sb transition does not overlap the Sn transition in n_e so that the Sb levels appear to lie 1 eV or more below the Sn levels. This places them near to or below the band bottom in the more dilute electron gases. Since full shells are normally lowered in progressively larger steps as Z increases, this indicates in turn that the Te $5p$ levels lie below the band bottom. Signs of an incipient resonance may also be apparent for In impurities in K, but the large σ_{SF} of In in Na shows that the levels remain well above E_F.

We have presumed in this discussion that the transition has a "one-electron" character, in which the $5p$ levels change position smoothly with composition, but an alternative "configurational" transition is also possible. For example, Ho in AgAl liquid solvents[6] undergoes a transition in which the two configurations of lowest energy are inverted as the host composition is varied, and the impurities change directly from one structure to the other without passing through intermediate stages. The data shown in Fig. 5 do not eliminate the possibility that the transition is substantially sharper than the solid line drawn through the points. It is worth noting also that solubility problems encountered here in NaK alloys near the transition are analogous to those met for rare earths in AgAl and CuAl near the configurational transition. The present results are not accurate enough to distinguish clearly between the two possibilities, but the ambiguity does not bear strongly on our subsequent discussion of ionicity outside the transitional region.

From the facts presented above we make the following quantitative estimates of the p-band location in K. With the band bottom at $E=0$ we have the Sb levels at 0 ± 1 eV, the Sn levels at $\frac{1}{2}E_F\pm1$ eV, and the In levels at $E_F+1\pm1$ eV. The sequence also indicates that the Te $5p$ levels lie perhaps 2 eV below the band bottom.

Figure 15 shows solid lines connecting the $5p$ orbital energies of Xe, I, Te, Sb, and Sn in K as calculated by Flynn and Lipari[11] using methods just mentioned. These levels were quoted with respect to the zero energy of freely propagating states in the ionic fields of the host lattice. When an average conduction-electron exchange is included to obtain correctly the location of band states, the conduction band falls between the levels indicated by the broken lines in Fig. 15. Correlation is neglected for both band states and core orbitals, and should largely cancel from the comparison of energies. The points in Fig. 15 are the energies just deduced for In, Sn, and Sb. When it is recognized that the theoretical values for Xe and I are rather reliable, one sees that the theory gives a very satisfactory account of the experimental results.

A simple insight into the causes that determine these energy levels may be obtained from the Wigner–Seitz model of metals. Suppose that we remove the ion and all electronic charge from one cell of potassium metal without modifying the electron distribution in the remaining lattice. Then the potential in the empty cell is roughly zero. A subsequent relaxation of the electron gas must leave the cell essentially empty, but it raises the potential energy of electrons in the cell by perhaps $E_F/2$, or about 1 eV. A Xe atom of atomic radius 2 Å placed in the empty cell of radius > 2.5 Å probably overlaps very little with the electron gas and simply has its one-electron valence levels raised from −11.4 to −10.4 eV. This level (~0.75 Ry) is very close to the theoretical result in Fig. 15. Similarly I, with an affinity of 3.3 eV, has one-electron levels at ~−2.3 eV in the cell. To neutralize the lattice, however, a screening charge of $|e|$ must be transported from the cell boundary to infinity thereby lowering the potential inside by $e^2/r_s\sim5$ eV and lowering the I^- $5p$ levels to ~−7 eV below vacuum level. This again is in excellent agreement with the precise theory. Several theoretical models discussed by other groups[12,15,32] have led to predictions that bear a qualitative re-

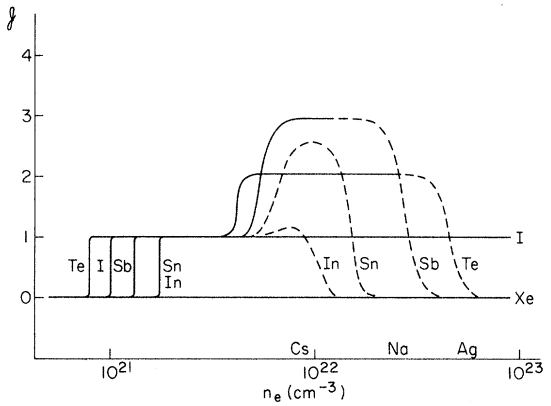

FIG. 16. Ionicity g, as defined in the text, of various Ag-row impurities shown as a function of electron density n_e, in monovalent metals. Bound levels are indicated by the solid lines and virtual levels by broken lines, but the boundaries are diffuse and have no sharp significance.

semblance to those deduced here, but that the models have contained features that make the results quantitatively unreliable.

We are now in a position to systematize our understanding of the ionic properties of Ag-row impurities in simple monovalent metals. The estimated ionicity is marked in Fig. 16 by solid lines for bound orbitals and by broken lines for resonant and virtual levels. As emphasized above, the boundary between these domains has no sharp significance. These trends were estimated from the present results for the range of metallic densities, and from the arguments presented in the Introduction for n_e small. In no case has any allowance been made for possible splitting of the $5p$ levels. We anticipate that similar trends emerge in other, less completely studied, rows of the Periodic Table, with changes that reflect the varying chemical properties. For example, the affinities of O and S are less than those of Se and Te, and a still greater disparity may appear in the second affinities. The $2p$ levels of O^{--} in metallic solution may therefore be unbound.

D. Noble-Metal Solvents

The behavior of Ag alloys at their melting transitions provides one of the most provocative results of this work. The magnetism of the noble metals themselves is, of course, not fully understood because of difficulties connected with the severe hybridization of the full shell of d orbitals into the conduction bands of the s-like valence states. Each of the noble metals undergoes a marked increase of diamagnetism at the melting point,[33] for reasons that again remain obscure. Presumably the hybridization is modified by liquification, through disordering and possibly by volume change also. Certainly, the susceptibility does not appear to be a function of volume alone throughout the accessible temperature range of the two phases. The solvent Knight shift K in Cu, which measures mainly the spin paramagnetism, has a substantial dependence on volume alone and is augmented at the melting transition by added changes that have been associated with Fermi-surface structure.[34] It is thought that the disappearance of p-like necks of the Fermi surface causes the s-wave density at E_F to increase and so increase the Knight shift,[34] although other views have also been published.[35]

An appearance of large anomalous electronic properties in solid-noble-metal alloys is itself a cause for surprise and concern. Solid-Ag alloys[36] and liquid-Cu alloys,[13] when probed by solvent NMR methods, yield very similar results that find a natural explanation inside the theory of impurity structure expounded here. Other bulk properties depend on averages that are in some degree independent of detailed impurity structure and are therefore susceptible to rigid-band arguments, but an explanation of the electronic specific heat of alloys, for example, requires details of the impurity density of states.[37] However, it is particularly curious that the [111] neck diameters on the Fermi surface of Cu alloys follow rigid-band predictions with surprising fidelity.[38] It is our belief that this result is the most pertinent to the anomalous impurity diamagnetism in solid-Ag alloys.

The large changes in impurity diamagnetism encountered in the melting transition might encourage alternative beliefs that they are associated either with the large volume change or with changes in the corelike d levels. Although the host lattice does suffer a large increase of diamagnetism at the transition, the first possibility can be eliminated immediately. The results of Henry and Rogers[21] show that the impurity diamagnetism depends almost wholly on impurity valence; the period dependence is much smaller despite large differences between the lattice dilatation caused by different impurities having a common Z. Nor can the impurity effects be ascribed to local perturbations of the solvent d-orbital diamagnetism, for the local dilatation would again provide an estimate of the overlap effects. Moreover, these effects would in part persist in the liquid, in direct contradiction with the experimental facts presented above.

For these reasons we are drawn back to the possibility that the observed impurity diamagnetism is associated with the necks on the Fermi surface. In this respect it is particularly important that the anomalous magnetism is observed in Cu alloys also,[21] for which the Fermi surface topology is very similar. Since the neck diameters in the alloys exhibit the impurity-valence dependence charac-

teristic of rigid-band effects, it appears reasonable that the susceptibility associated with orbits over the necks should also do so. Also in favor of this argument is the fact that Landau diamagnetism is temperature independent and does not depend on the electron lifetimes being long enough to make the Landau levels clearly resolved. Again, the abrupt disappearance of the diamagnetism at the melting transition is precisely what one would anticipate from the isotropy of the liquid phase and the consequent disappearance of the Fermi-surface necks. We therefore agree with the suggestion of Kohn and Luming[23] that the effects must find their origin in the band structure. We believe that the p-like necks on the Fermi surface may be the structural link that introduces the diamagnetism and its observed dependence on impurity valence.

With the advantage of hindsight one can see that these effects are to be expected for materials with more sensitive Fermi-surface structures, if not for the noble metals. Bi, for example, has a small Fermi surface that gives rise to a large diamagnetism. One cannot doubt that solutes may have enormous impurity magnetism in Bi, because small numbers of added electrons can make large fractional changes in the host magnetism. Moreover, Bi is a perfectly good metal in the liquid phase, and the large impurity susceptibilities must disappear. The analogy between this example and the experimental results for Ag alloys is therefore exact.

In concluding, we emphasize that this is a fascinating problem. The diamagnetism introduced by the Fermi-surface necks in solid noble metals and their dilute alloys deserves the attention of an expert theorist, concerned with transport properties.

ACKNOWLEDGMENTS

The authors wish to thank M. D. Mikolosko for assistance with the work on NaK Alloys, J. J. Peters for advice in connection with the specimen holders, and C. P. Slichter and his group for many stimulating discussions of their spin-flip-scattering work.

---

*Research supported in part by the National Science Foundation Grant No. GH-33634 and in part by the Advanced Research Projects Agency under Contract No. HC-15-67-C-0221.

†Present address: Center for Tectonophysics, Texas A & M University, College Station, Texas 77843.

[1]J. A. Rigert and C. P. Flynn, Phys. Rev. Letters 26, 1177 (1971); C. P. Flynn and N. O. Lipari, Phys. Rev. Letters 27, 1365 (1971); M. D. Mikolosko, J. A. Rigert, and C. P. Flynn, Physics Letters 38, 69 (1972); C. P. Flynn, Physics Letters 41, 45 (1972).

[2]See N. F. Mott and H. Jones, *Electronic Structure of Metals and Alloys* (Oxford U. P., London, 1936).

[3]For a general discussion of impurity structure see C. P. Flynn, *Point Defects and Diffusion* (Oxford U. P., London, 1972), p. 741-77.

[4]See, for example, the review by M. A. Bredig, in *Molten Salt Chemistry*, edited by M. Blander (Interscience, New York, 1964).

[5]R. Haensel, G. Keitel, B. Sonntag, C. Kunz, and P. Schreiber, Phys. Stat. Sol. 42, 85 (1970); for early work see J. A. Bearden and A. F. Burr, Rev. Mod. Phys. 39, 125 (1967).

[6]J. A. Rigert and C. P. Flynn, Phys. Rev. B 5, 4569 (1972).

[7]J. J. Peters and C. P. Flynn, Phys. Rev. (to be published).

[8]G. W. Stupian and C. P. Flynn, Phil. Mag. 17, 295 (1968).

[9]This idea was first suggested for the ground state by J. M. Ziman, Adv. in Physics 13, 89 (1964).

[10]See L. Hedin and S. Lundquist, in *Solid State Physics* (Academic, New York, 1969), Vol. 23.

[11]C. P. Flynn and N. O. Lipari, Phys. Rev. B 7, 2215 (1973).

[12]J. R. Asik, M. A. Ball, and C. P. Slichter, Phys. Rev. 181, 645 (1969); M. A. Ball, J. R. Asik, and C. P. Slichter, Phys. Rev. 181, 662 (1969); E. K. Cornell and C. P. Slichter, Phys. Rev. 180, 358 (1969).

[13]R. L. Odle and C. P. Flynn, Phil. Mag. 16, 699 (1966); D. A. Rigney and C. P. Flynn, Phil. Mag. 15, 1213 (1967).

[14]See Ref. 13 and J. Heighway and E. F. W. Seymour, Physics Letters 29, 282 (1969).

[15]See Ref. 12 and R. A. Ferrell and R. E. Prange, Phys. Rev. Letters 17, 163 (1966).

[16]J. J. Peters, thesis (University of Illinois, 1971) (unpublished).

[17]M. Hansen, *Constitution of Binary Alloys* (McGraw-Hill, New York, 1958); R. P. Elliott, *Constitution of Binary Alloys* (McGraw-Hill, New York, 1965).

[18]R. Bowers, Phys. Rev. 100, 1140 (1955).

[19]E. W. Collings, J. Phys. Chem. Solids 26, 949 (1965).

[20]B. Bohm and W. Klemm, Z. Anorg. U. Allgem. Chem. 243, 69 (1939); K. Venkateswarlu and S. Srirman, Z. Naturforsch. 13a, 455 (1958).

[21]W. G. Henry and J. L. Rogers, Can. J. Phys. 38, 908 (1960); for additional results on Cu alloys see also Phil. Mag. 1, 239 (1965).

[22]For a recent review see D. G. Graham and N. H. March, Crys. Lattice Defects 1, 121 (1970).

[23]W. Kohn and M. Luming, J. Phys. Chem. Solids 24, 851 (1963).

[24]This approach originated in various papers by J. Friedel and his co-workers. The area is reviewed in Ref. 3.

[25]See J. Friedel, Adv. in Phys. 3, 446 (1954).

[26]R. Harrison, Phil. Mag. 22, 131 (1970).

[27]P. W. Anderson, Phys. Rev. 124, 41 (1961).

[28]This area is reviewed by J. Kondo and by A. J. Heeger, in *Solid State Physics* (Academic, New York, 1969), Vol. 23.

[29]See *Landolt-Börnstein Tables* (Springer, Berlin, 1967), Vol. II, p. 9.

[30]W. Kohn and C. Majumdar, Phys. Rev. 138, A1617

(1965).
[31]N. F. Mott, J. Phys. (Paris) 23, 594 (1962).
[32]S. D. Mahanti and F. Toigo, Physics Letters 36A, 61 (1971).
[33]See Ref. 29, and, for Cu, J. Bensel and J. A. Gardner, J. Appl. Phys. 41, 1157 (1970).
[34]R. L. Odle and C. P. Flynn, Phys. Rev. B 4, 3246 (1971).
[35]U. El-Hanany and D. Zamir, Phys. Rev. 183, 809 (1969).
[36]T. J. Rowland, Phys. Rev. 125, 459 (1962).
[37]These matters are discussed in Ref. 3.
[38]L. F. Chollet and I. M. Templeton, Phys. Rev. 170, 656 (1968).